International Journal of Biological Macromolecules 182 (2021) 1906–1914

Contents lists available at ScienceDirect

International Journal of Biological Macromolecules

journal homepage: http://www.elsevier.com/locate/ijbiomac

Solvent-induced conformational tuning of lysozyme protein adlayers on silica surfaces: A QCM-D and LSPR study

Bo Kyeong Yoon [a,1], Gamaliel Junren Ma [b,1], Hyeonjin Park [a,b], Abdul Rahim Ferhan [b], Nam-Joon Cho [b,*], Joshua A. Jackman [a,*]

[a] School of Chemical Engineering, Sungkyunkwan University, Suwon 16419, Republic of Korea
[b] School of Materials Science and Engineering, Nanyang Technological University, 639798, Singapore

ARTICLE INFO

Article history:
Received 16 February 2021
Received in revised form 13 May 2021
Accepted 16 May 2021Available online 19 May 2021

Keywords:
Lysozyme
Protein adsorption
Conformational stability

ABSTRACT

There is broad interest in functionalizing solid surfaces with lysozyme, which is a widely studied antimicrobial protein. To date, most efforts have focused on developing more effective immobilization schemes to promote lysozyme attachment in fully aqueous conditions, while there remains an outstanding need to understand how tuning the solution-phase conformational stability of lysozyme proteins can modulate adsorption behavior and resulting adlayer properties. Inspired by the unique conformational behavior of lysozyme proteins in water-ethanol mixtures, we conducted quartz crystal microbalance-dissipation (QCM-D) and localized surface plasmon resonance (LSPR) measurements to systematically investigate the adsorption behavior of lysozyme proteins onto silica surfaces across a wide range of water-ethanol mixtures. Our findings revealed that lysozyme adsorption behavior strongly depended on the ethanol fraction in a non-monotonic fashion and this trend could be rationalized by taking into account how competing effects of water and ethanol solvation influence solution-phase protein size and conformational stability. Integrated analysis of the QCM-D and LSPR measurement trends enabled quantitative determination of the solvent mass within lysozyme adlayers, which tended to decrease at higher ethanol fractions and supported that the hydrodynamic properties of lysozyme adlayers are mainly influenced by the degree of protein conformational flexibility as opposed to solvation effects alone.

1. Introduction

The noncovalent adsorption of biological macromolecules such as proteins and peptides onto solid surfaces is pertinent to various applications, including biosensors [1,2], drug delivery [3,4], and enzyme catalysis [5,6]. Within this scope, there has long been interest in scrutinizing how various parameters affect protein adsorption behavior [7–9] as well as in translating fundamental knowledge into advanced design strategies such as the nanoarchitectonics concept to precisely control the fabrication of protein-coated surfaces [10,11]. While it is widely investigated how protein adsorption depends on protein-surface interactions, which can be tuned based on material properties of the solid support (*e.g.*, atomic composition, surface charge, and topography [12–15]), another important, yet often underappreciated factor is the conformational properties of the protein structure itself, which are closely related to the strength of intramolecular interactions within the protein and affect the extent of adsorption-related protein unfolding [16–18].

In recent years, there has been extensive interest in understanding how the solution-phase conformational properties of proteins affect adsorption behavior as mounting evidence indicates that such issues are important not only for fundamental knowledge but also for practical applications such as antifouling coatings. An early study demonstrated how engineered variants of a human enzyme with greater conformational stabilities underwent less irreversible adsorption on various solid surfaces [19]. Building on this concept, another study compared the adsorption behavior of bovine serum albumin (BSA) protein with human and rat protein analogues and demonstrated that BSA had the lowest solution-phase conformational stability and underwent the greatest extent of denaturation in the adsorbed state [20]. Moreover, BSA has been used as a model protein to study how environmental conditions such as ionic strength and temperature as well as how the presence of amphipathic stabilizers such as fatty acids and monoglycerides can influence protein conformational stability and resulting adsorption behavior and coating performance [21–24]. It has also been observed that the solvent environment has a significant effect on solution-phase conformational stability, and BSA proteins in water-ethanol mixtures can exhibit increased conformational flexibility that leads to the formation of denser protein adlayers [25,26]. This latter finding emphasizes the importance of not only stabilizing protein secondary structure but

* Corresponding authors.
E-mail addresses: njcho@ntu.edu.sg (N.-J. Cho), jjackman@skku.edu (J.A. Jackman).
[1] These authors contributed equally to this work.

https://doi.org/10.1016/j.ijbiomac.2021.05.113
0141-8130/

also intentionally modulating, and in some cases destabilizing, protein conformational properties *via* the solvent environment to tailor the molecular-level properties of protein-based coatings.

From a macromolecular perspective, it is important to extend such investigations to other proteins with distinct physiochemical features and one promising candidate is the antimicrobial lysozyme protein. While lysozyme's antimicrobial activity stems from its ability to catalyze the hydrolysis of glycosidic bonds in bacterial cell walls, it also demonstrates a lectin-like ability to bind to carbohydrates, which suggests its involvement in the immune system as well [27]. Indeed, such biological activities have contributed to the growing interest in controlling lysozyme adsorption to fabricate protein-coated antimicrobial surfaces [28–31] and to functionalize nanoparticle surfaces [32,33]. To date, the effects of various experimental parameters, such as temperature, solution pH, ionic strength, and protein concentration, on lysozyme adsorption onto solid surfaces in fully aqueous environments has been extensively studied [34–37]. In addition to its adsorption properties, the solution-phase properties of lysozyme, such as its propensity for oligomerization and fibrillation in certain conditions, have been studied using various techniques, including nuclear magnetic resonance (NMR) spectroscopy, X-ray crystallography, light scattering, and molecular modeling [38–40]. Within this latter scope, it has also been established that the addition of organic solvents such as ethanol to aqueous lysozyme solutions can impact solution-phase conformational stability [41,42]. Interestingly, due to these conformational changes and competing solvent interactions, recent findings have shown that the molecular size of monomeric lysozyme proteins in water-ethanol mixtures tends to oscillate by over two-fold (1.3- to 2.9-nm hydrodynamic radius) with increasing ethanol fraction [43]. This oscillatory trend in lysozyme size is distinct from the monotonic size behavior of BSA in water-ethanol mixtures (*i.e.*, stable BSA monomer size until aggregation commences at and above a critical ethanol fraction [26]) and thus motivates investigating lysozyme adsorption onto solid surfaces across a range of water-ethanol mixtures.

Herein, we conducted quartz crystal microbalance-dissipation (QCM-D) and localized surface plasmon resonance (LSPR) experiments to track lysozyme adsorption onto silica surfaces in water-ethanol mixtures ranging from 0 to 40% (*v*/*v*) ethanol in 10% increments. Particular focus was placed on scrutinizing the adsorption kinetics and final adlayer properties in terms of optical, acoustic, and solvent masses in order to rationalize how tuning the ethanol fraction in water-ethanol mixtures influences not only solution-phase lysozyme conformational properties but also dictates the formation of precisely controlled lysozyme adlayers.

2. Materials and methods

2.1. Protein sample preparation

Lysozyme from chicken egg white (L6876) was obtained in lyophilized powder form from Sigma-Aldrich (USA). Water-ethanol mixtures from 0 to 40% (*v*/*v*) in 10% increments were prepared by using Milli-Q deionized water (MilliporeSigma, USA). Protein powders were dissolved in the water-ethanol mixtures to a bulk protein concentration of 0.72 mg/mL (50 μM) and filtered through a polyethersulfone membrane filter with 0.2-μm diameter pores (Thermo Fisher Scientific, catalog no. 595–4520) and stored at 4 °C until use.

2.2. Quartz crystal microbalance-dissipation (QCM-D)

QCM-D measurements were conducted using a QSense E4 instrument (Biolin Scientific AB, Sweden) with silica-coated AT-cut quartz crystal sensor chips (QSX 303, Biolin Scientific AB). Before experiment, the sensor chips were sequentially rinsed with 1% (*w*/*v*) aqueous sodium dodecyl sulfate (SDS) solution, deionized water, and ethanol, followed by nitrogen gas drying. The sensor chips were then treated with oxygen plasma for 1 min at 50 W radiofrequency power by using a CUTE-1MPR machine (Femto Science Inc., Hwaseong, Republic of Korea). A peristaltic pump (Reglo Digital MS-4/6, Ismatec, Glattbrugg, Switzerland) was used to inject liquid samples into the measurement chamber at a flow rate of 50 μL/min. The resonance frequency (Δf) and energy dissipation (ΔD) shifts were recorded as a function of time with a time resolution of 0.9 Hz. Data collection was controlled using the QSoft software program (Biolin Scientific AB) and data processing was conducted using the Q-Tools (Biolin Scientific AB) and OriginPro (OriginLab, Northampton, MA) software programs. All measurements were conducted at 25 °C and the normalized data at the fifth overtone are reported. The rates of change of resonance frequency ($d\Delta f/dt$) were obtained by calculating the first-order time derivative.

2.3. Localized surface plasmon resonance (LSPR) sensing

LSPR experiments were conducted using an Insplorion XNano instrument (Insplorion AB, Sweden) in optical transmission mode with sensor chips consisting of embedded silver nanodisk transducers on a fused silica substrate with a 10 nm-thick silicon nitride coating. Before experiments, the sensor chips were sequentially rinsed with 1% (*w*/*v*) aqueous sodium dodecyl sulfate (SDS) solution, deionized water, and ethanol, followed by nitrogen gas drying. The sensor chips were then treated with oxygen plasma for 1 min at 50 W radiofrequency power by using a CUTE-1MPR machine (Femto Science Inc.), which resulted in the formation of a silica overlayer on the sensor surface. A peristaltic pump (Reglo Digital MS-4/6, Ismatec) was used to inject liquid samples into the measurement chamber at a flow rate of 50 μL/min. The peak of the optical extinction spectrum was calculated based on centroid analysis [44] and the peak shifts ($\Delta\lambda$) were recorded with a time resolution of 1 Hz. Data collection and processing were controlled using the Insplorer (Insplorion AB) and OriginPro (OriginLab) software programs, respectively. The rates of change of peak shift ($d\Delta\lambda/dt$) were obtained by calculating the first-order time derivative.

3. Results and discussion

3.1. Measurement strategy

As a model protein, we selected lysozyme, which is a widely studied antimicrobial protein that typically has a net positive charge (isoelectric point: ~11.4) and relatively high conformational stability [45]. The basic experimental strategy is presented in Fig. 1A and involved tracking lysozyme adsorption onto silica surfaces in different water-ethanol mixtures by QCM-D and LSPR measurements. As mentioned above, it has been reported that lysozyme exhibits oscillatory size trends as a function of ethanol fraction in water-ethanol mixtures [43] and such variations are expected to influence the adsorption kinetics and adlayer properties.

QCM-D experiments were conducted using silica-coated sensor chips, whereby real-time shifts in the resonance frequency (Δf) and energy dissipation (ΔD) signals were tracked and reflect the mass and viscoelastic properties of the protein adlayer, respectively. Quantitatively, a negative Δf shift indicates mass adsorption while a positive ΔD shift indicates greater viscoelastic character of an adsorbate. A representative QCM-D measurement protocol is presented in Fig. 1B and consists of the following stages: (i) an initial baseline in water was established; (ii) the appropriate water-ethanol mixture was introduced; (iii) 50 μM lysozyme in the equivalent water-ethanol mixture was added under continuous flow conditions; (iv) a washing step was conducted using the same water-ethanol mixture without protein; and (v) another washing step was conducted using water alone. Note that the difference in the signal responses between stages i and ii is due to the difference in the viscosity and density between water and the water-ethanol solvent mixture rather than due to protein adsorption. As such, we focused on analyzing measurement shifts related to protein adsorption in a solvent

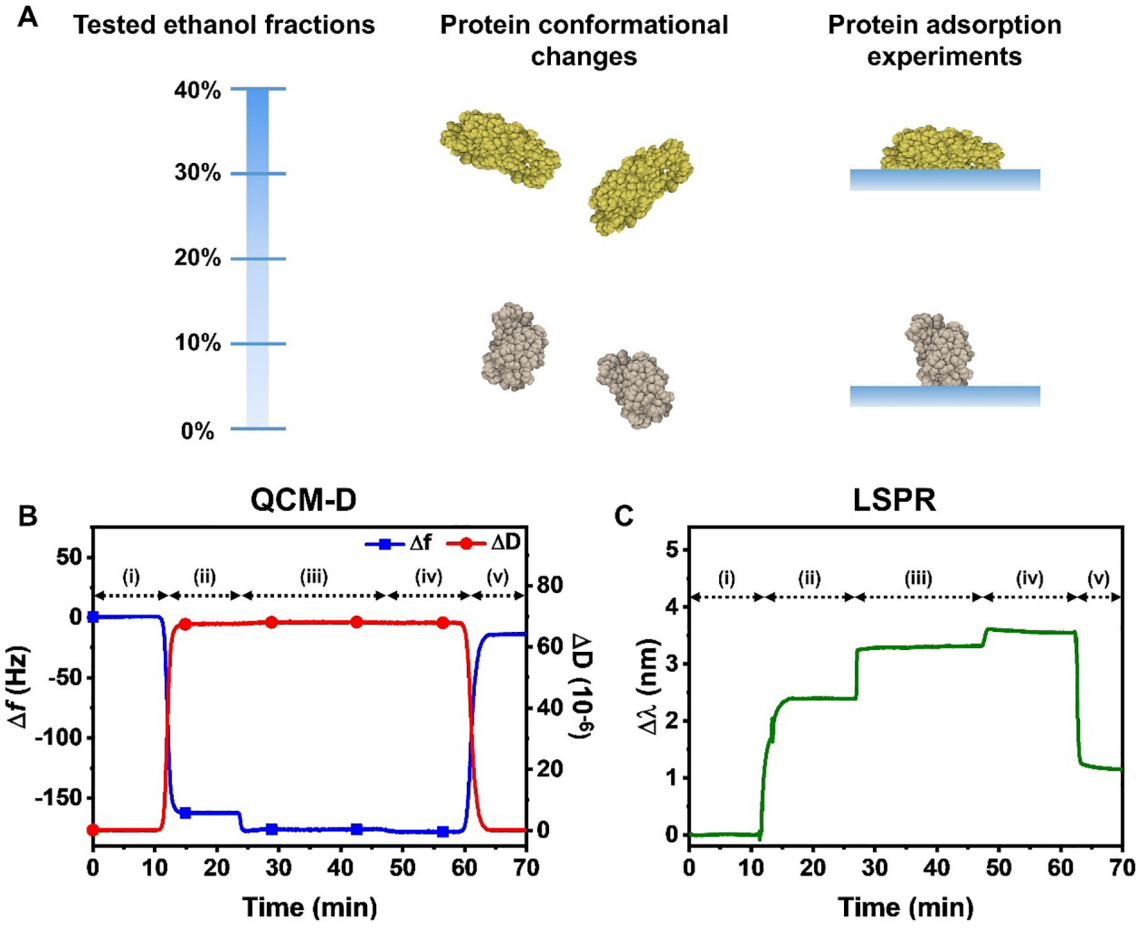

Fig. 1. Experimental strategy for tracking lysozyme adsorption in water-ethanol mixtures. (A) Overview of the study design. The lysozyme protein structure was rendered from Protein Data Bank (PDB) file 1IEE. (B, C) Representative graphs for (B) QCM-D and (C) LSPR experimental protocols to track lysozyme adsorption in water−ethanol mixtures with 40% (*v*/*v*) ethanol. In panel (B), the Δ*f* and ΔD signals are distinguished by square and circle symbol markers, respectively. QCM-D and LSPR experimental protocols consisted of the following stages: (i) water baseline; (ii) exchange to the appropriate water−ethanol mixture; (iii) exchange to the equivalent water−ethanol mixture containing 50 μM lysozyme; (iv) wash with the equivalent water−ethanol mixture (without protein); and (v) wash with water. All steps were performed under continuous flow conditions with brief pause for solvent exchange.

vs. the baseline signal in equivalent solvent without protein. More specifically, the following three sets of protocol steps were analyzed: (1) protein adsorption in the water-ethanol mixture *before* solvent washing relative to the corresponding baseline in the equivalent water-ethanol mixture (stages ii *vs.* iii), (2) protein adsorption *after* solvent washing relative to the corresponding baseline in the equivalent water-ethanol mixture (stages ii *vs.* iv), and (3) protein adsorption uptake after water washing relative to the initial baseline in water (stages i *vs.* v).

We also conducted LSPR experiments using a sensor chip that had a silica-coated array of plasmonic silver nanodisks to track the real-time shifts in the optical extinction peak wavelength (Δλ) due to changes in the local refractive index near the sensor surface, which were related to lysozyme adsorption. While the QCM-D technique is sensitive to adsorbed protein mass and hydrodynamically-coupled solvent mass, a noteworthy aspect of the LSPR technique is that it is sensitive to adsorbed protein mass only along with related conformational changes. As such, a larger Δλ shift typically indicates a greater "dry" mass of adsorbed proteins and/or the proteins adsorbing, on average, closer to the sensor surface. A representative LSPR measurement protocol is presented in Fig. 1C, which mirrors the QCM-D protocol and the same three sets of protocol steps were analyzed as described above for the QCM-D experiments.

Before proceeding to discuss the QCM-D and LSPR adsorption measurements, we first provide more specific information about the experimentally observed oscillatory trend in lysozyme size in water-ethanol mixtures as a function of ethanol fraction. Chattoraj et al. reported that the lysozyme diameter in water-ethanol mixtures with 0, 9, 19.5, 32.5, and 38% ethanol fractions was 3.8, 4.2, 3.4, 5.2, and 4.4 nm, respectively [43]. Hence, to a first approximation, these data support that the lysozyme size tends to oscillate back and forth in magnitude across the range of 0–40% ethanol fractions used in this study.

3.2. QCM-D measurements

Real-time QCM-D Δ*f* and ΔD signals for lysozyme adsorption kinetics in different water-ethanol mixtures are presented in Fig. 2A, B. After establishing a stable baseline signal in the appropriate water-ethanol mixture, 50 μM lysozyme in the equivalent water-ethanol mixture was added (see first arrow), followed by a washing step (see second arrow). In general, the measurement responses showed rapid, one-step kinetics until adsorption saturation was reached, which is likely due to strong electrostatic attraction between positively charged lysozyme (isoelectric point around pH 11; see Ref. [46]) and the negatively charged silica surface (isoelectric point around pH 3.9; see Ref. [47]). Notably, the magnitudes of the Δ*f* and ΔD shifts depended on the ethanol fraction in a non-monotonic manner.

In 0% ethanol, lysozyme adsorption yielded Δ*f* and ΔD shifts of -15.2 ± 0.5 Hz and $0.22 \pm 0.12 \times 10^{-6}$, respectively, at saturation. In 10% ethanol, larger Δ*f* and ΔD shifts of -17.6 ± 0.3 Hz and $0.96 \pm 0.06 \times 10^{-6}$, respectively, were observed and indicate greater adsorption uptake. On the other hand, in 20% ethanol, noticeably smaller Δ*f*

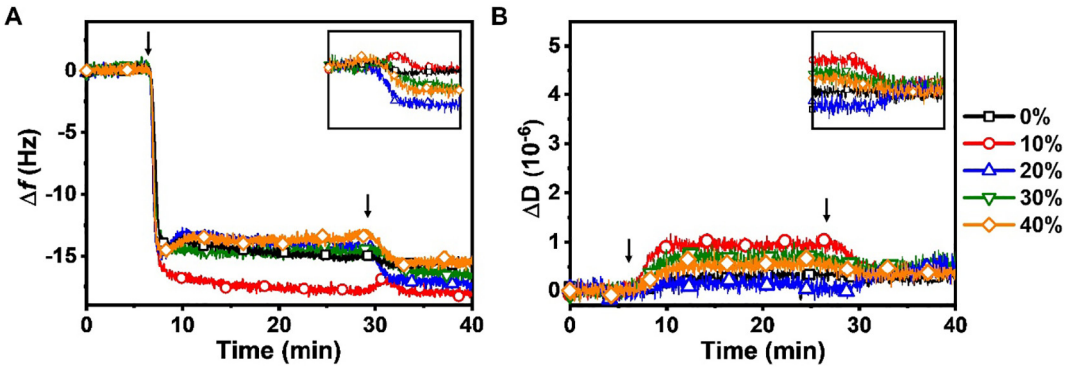

Fig. 2. QCM-D tracking of lysozyme adsorption in water-ethanol mixtures. (A) Time-resolved Δf shifts for lysozyme adsorption onto a silica surface in different water-ethanol mixtures as a function of ethanol fraction. The baseline was recorded in the appropriate water-ethanol mixture, followed by 50 μM lysozyme addition from $t = 5$ min onwards and then a washing step in the equivalent water-ethanol mixture (without protein) from $t = 25$ min. The inset shows a magnified view of the normalized Δf shifts due to solvent washing. (B) Corresponding data for the time-resolved ΔD shifts that were measured simultaneously in the QCM-D measurements.

and ΔD shifts of -14.4 ± 0.1 Hz and $0.05 \pm 0.04 \times 10^{-6}$, respectively, were obtained, while, in 30% ethanol, relatively larger Δf and ΔD shifts of -15.1 ± 0.2 Hz and $0.66 \pm 0.03 \times 10^{-6}$, respectively, were again observed. In 40% ethanol, the corresponding Δf and ΔD shifts were -13.9 ± 0.1 Hz and $0.50 \pm 0.04 \times 10^{-6}$, respectively. Together, these data support that adsorbed lysozyme proteins form a protein monolayer on the silica surface on account of the adsorbed mass density (~260 ng/cm^2) and relatively small ΔD shifts ($<1 \times 10^{-6}$) [37]. Another interesting observation is that the magnitudes of the Δf and ΔD shifts tended to oscillate up and down as the ethanol fraction in the water-ethanol mixture was varied in 10% increments, whereby larger responses corresponded to solvent conditions in which solution-phase lysozyme proteins had a relatively larger hydrodynamic diameter and *vice versa*.

Upon solvent washing with the equivalent water-ethanol mixture (without protein), the adsorbed lysozyme proteins underwent modest structural rearrangement, which was also captured in the Δf and ΔD signals. In 0–10% ethanol, the Δf shift increments due to solvent washing were nearly negligible (<-1 Hz) while larger shift increments of around -1 to -3 Hz were observed in 20–40% ethanol (see Fig. 1A inset). Together with experimentally observed drops in the corresponding ΔD shifts, these findings support that the lysozyme adlayers in 20–40% ethanol underwent densification upon solvent washing. These findings are striking because solvent washing typically induces protein desorption as opposed to densification, providing further evidence of strong protein-surface interactions in this system.

The QCM-D measurement trends are summarized in Fig. 3. For lysozyme adsorption in water-ethanol mixtures, the corresponding Δf and ΔD shifts *before* solvent washing both indicate oscillatory behavior as a function of ethanol fraction (Fig. 3A). While the variation in the Δf shift magnitudes was relatively small, a clear trend was observed and more pronounced variation in the ΔD shift magnitudes was also observed. These trends agree well with the reported trend in the hydrodynamic diameter of solution-phase lysozyme proteins, supporting that protein conformational flexibility and its dependence on the solvent condition plays an important role in dictating the adlayer properties.

Fig. 3B shows the Δf and ΔD shifts for lysozyme adsorption *after* solvent washing relative to the initial signal in the equivalent water-ethanol mixture prior to protein addition. The Δf shifts were relatively small and similar, reflecting that solvent washing tended to have negligible effect in the 0–10% ethanol range while causing a modest additional decrease in the 20–40% ethanol range due to protein densification. Likewise, the ΔD shifts tended to decrease in most cases and the final values were quite small, indicating rigid attachment to the silica surface. The only exception was lysozyme adsorption in 20% ethanol, in which case solvent washing led to a larger ΔD shift and might relate to an increase in ethanol solvation as competing protein-water and protein-ethanol interactions are particularly significant around this solvent condition [43].

We also plotted the final Δf and ΔD shifts after a subsequent water washing step relative to the initial baseline in water at the beginning of the experiment (Fig. 3C). The final Δf shifts were in the range of -15 to -19 Hz and the largest values were observed for lysozyme adlayers in the 20–30% ethanol range. The results indicate tight coupling of the lysozyme adlayers to the silica surfaces while the comparatively

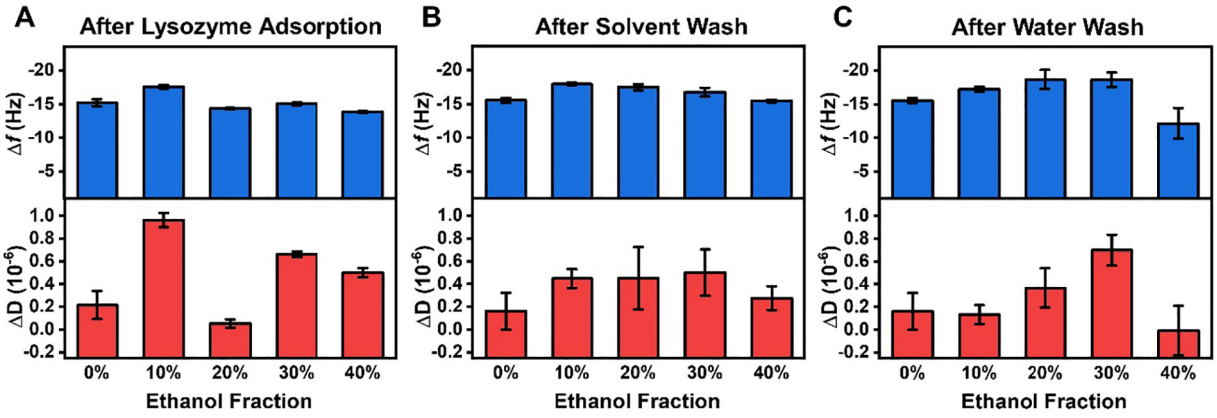

Fig. 3. Summary of QCM-D results for lysozyme adsorption in water-ethanol mixtures. The Δf and ΔD shifts are reported for (A) lysozyme adlayer in water-ethanol mixture *before* solvent washing (relative to baseline in the appropriate water-ethanol mixture), (B) lysozyme adlayer in water-ethanol mixture *after* solvent washing (relative to baseline in the appropriate water-ethanol mixture), and (C) lysozyme adlayer *after* water washing (relative to baseline in water). Data are reported as mean ± standard deviation (s.d.) for $n = 3$ replicates.

larger ΔD shift in the 30% ethanol condition supports that the lysozyme adlayer in that case exhibited relatively greater viscoelastic properties.

3.3. LSPR measurements

The corresponding LSPR measurement data for lysozyme adsorption kinetics in different water-ethanol mixtures are presented in Fig. 4A. While the QCM-D measurements are sensitive to adsorbed protein mass and hydrodynamically-coupled solvent mass, the LSPR measurements are sensitive to adsorbed protein mass only, which provides a complementary viewpoint to characterize adlayer properties. After establishing a stable baseline signal in the appropriate water-ethanol mixture, 50 μM lysozyme in the equivalent water-ethanol mixture was added (see first arrow), followed by a washing step (see second arrow). In line with the QCM-D results, the LSPR measurement responses also showed rapid, one-step kinetics until adsorption saturation was reached while the Δλ shift values tended to increase moderately at higher ethanol fractions. In 0% ethanol, lysozyme adsorption yielded a Δλ shift of 0.73 nm and the corresponding Δλ shifts in 10% and 20% ethanol were 0.82 and 0.81 nm, respectively. Lysozyme adsorption in 30% ethanol yielded the largest Δλ shift of 1.04 nm while the corresponding Δλ shift in 40% ethanol decreased slightly, but was still relatively high, to 0.93 nm.

Closer inspection of the solvent washing step showed that this process involves reconfiguration of adsorbed lysozyme molecules in most cases (Fig. 4B). In 0% ethanol, solvent washing led to a small, multi-step response, resulting in a final Δλ shift increment of 0.02 nm. By contrast, solvent washing led to sharp increases in the Δλ signal in the other cases and the corresponding Δλ shift increments in 10% and 20% ethanol were 0.24 and 0.26 nm, respectively. In 30% ethanol, there was an even larger Δλ shift increase of 0.38 nm, while the Δλ shift increase was 0.27 nm in 40% ethanol. Since the LSPR measurement response is sensitive to the amount and conformational properties of adsorbed proteins and not sensitive to hydrodynamically coupled solvent, the positive Δλ shift increments support adlayer densification and it is also noteworthy that the magnitudes of the Δλ shift increases upon solvent washing are relatively larger than the magnitudes of the corresponding QCM-D responses discussed above.

The LSPR measurement trends are summarized in Fig. 5. For lysozyme adsorption in water-ethanol mixtures, the corresponding Δλ shifts *before* solvent washing show a modest increase as a function of ethanol fraction (Fig. 5A). The largest Δλ shift occurred in the 30% ethanol condition. These data support that, with increasing ethanol fraction, adsorbed lysozyme proteins are more deformed on the sensor surface. The surface coverage of adsorbed lysozyme proteins was also calculated based on the LSPR measurement responses in different water-ethanol mixtures and the fractional surface coverage increased from ~0.35 in 0% ethanol to ~0.53 in 40% ethanol (see Supplementary Material for calculation details). The maximum surface coverage was ~0.56 in 30% ethanol. Similar trends were also observed for the Δλ shifts *after* solvent washing relative to the initial signal in the equivalent water-ethanol mixture prior to protein addition, as well as for the Δλ shifts after a subsequent water washing step relative to the initial baseline in water at the beginning of the experiment (Fig. 5B, C).

3.4. Mass characterization of lysozyme adlayers

We further analyzed the QCM-D and LSPR data to calculate the acoustic, optical, and solvent mass properties of the lysozyme adlayers in the different water-ethanol mixtures. Since the lysozyme adlayers exhibited relatively low ΔD shifts ($<1 \times 10^{-6}$) in all QCM-D experiments, the acoustic mass values of the lysozyme adlayers – encompassing the mass of adsorbed protein molecules plus hydrodynamically-coupled solvent molecules – were estimated by using the Sauerbrey equation, which converts the Δ*f* shifts into areal mass density values [48]. On the other hand, the optical mass values of the lysozyme adlayers (protein mass only without coupled solvent mass) were calculated from LSPR data by using the Lorentz-Lorenz equation (see Supplementary Material for calculation details) [49–51]. The hydrodynamically-coupled solvent mass within the lysozyme adlayers was then determined by calculating the difference between the acoustic and optical mass values in each water-ethanol mixture. A summary of the acoustic, optical, and solvent mass values for the lysozyme adlayers is presented in Fig. 6.

In general, the amount of solvent mass within the lysozyme adlayer showed a tendency to decrease at higher ethanol fractions across all the test stages within the adsorption protocol (Fig. 6A–C). This tendency agrees well with the larger Δλ shifts observed in the LSPR experiments at higher ethanol fractions and supports that lysozyme proteins undergo greater adsorption-related denaturation and have higher surface coverages to form denser, protein-rich adlayers at higher ethanol fractions. In another study involving multiple surface-sensitive measurement techniques, Komorek et al. investigated lysozyme adsorption onto a gold surface as a function of protein concentration [52]. In that study, the QCM-D technique was utilized together with the surface plasmon resonance (SPR) technique, which is another type of label-free optical sensor with a longer penetration depth than the LSPR technique. Similar to our findings, the authors reported that a decrease in the amount of protein adlayer hydration is due to an increase in the lysozyme adlayer surface coverage, although that finding was discussed within the context of an increase in solution-phase bulk protein concentration and consequently, a faster rate of diffusion-limited protein adsorption to the gold surface. By contrast, in our study, the reduced solvent mass and increased surface coverage occurs due to ethanol-induced changes in the conformational flexibility of lysozyme protein molecules. Of note, the trend in solvent mass for lysozyme adlayers

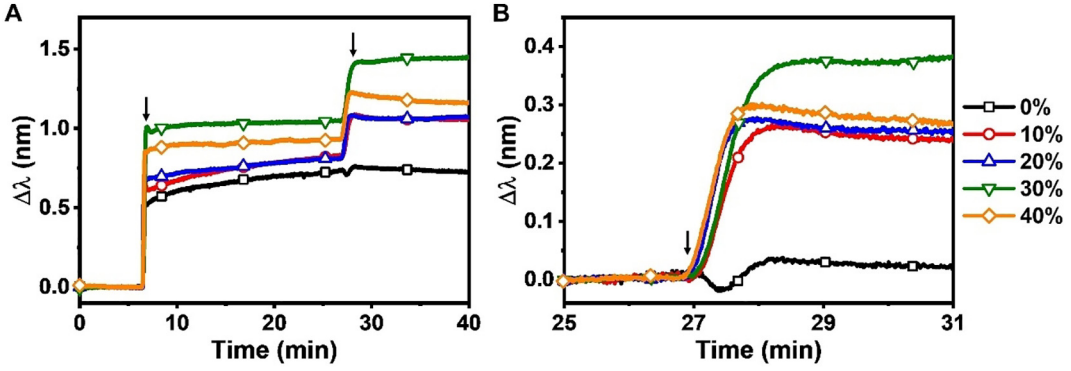

Fig. 4. LSPR tracking of lysozyme adsorption in water-ethanol mixtures. (A) Time-resolved Δλ shifts for lysozyme adsorption onto a silica-coated nanodisk surface in different water-ethanol mixtures as a function of ethanol fraction. The baseline was recorded in the appropriate water-ethanol mixture, followed by 50 μM lysozyme addition from $t = 5$ min onwards and then a washing step in the equivalent water-ethanol mixture (without protein) from $t = 25$ min. (B) Magnified view of the normalized Δλ shifts due to solvent washing.

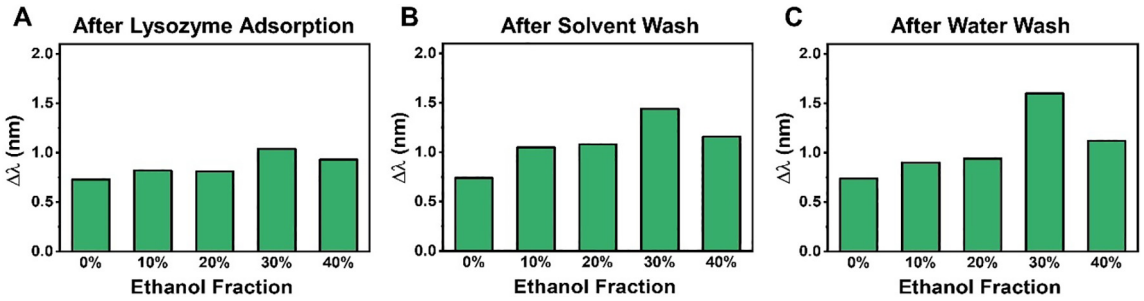

Fig. 5. Summary of LSPR results for lysozyme adsorption in water-ethanol mixtures. The Δλ shifts are reported for (A) lysozyme adlayer in water-ethanol mixture *before* solvent washing (relative to baseline in the appropriate water-ethanol mixture), (B) lysozyme adlayer in water-ethanol mixture *after* solvent washing (relative to baseline in the appropriate water-ethanol mixture), and (C) lysozyme adlayer *after* water washing (relative to baseline in water).

before solvent washing (*cf.* Fig. 6A) is distinct from the pronounced oscillatory trend in ΔD shifts for lysozyme adlayers *before* solvent washing (*cf.* Fig. 3A), which additionally supports that the oscillatory response behavior originates from variations in lysozyme adlayer properties – reflective of changes in protein size and conformational flexibility in different water-ethanol mixtures – as opposed to variations in solvent mass alone.

3.5. Lysozyme adsorption kinetics

We also evaluated lysozyme adsorption kinetics by calculating the time derivatives of the Δ*f* and Δλ shift responses from the QCM-D and LSPR measurement data, respectively. The corresponding data are presented in Fig. 7A, B. Since protein adsorption occurs in the diffusion-limited regime, the experimentally measured rates reflect the net rate of protein molecules contacting the sensor surface (adsorption rate minus desorption rate) plus the extent of adsorption-related protein denaturation [20,22,26]. As such, larger values of the $|d\Delta f/dt|$ and $d\Delta\lambda/dt$ signals indicate a greater degree of adsorption irreversibility and/or more extensive, adsorption-related denaturation. Since the probing volume of the LSPR technique is much smaller than that of the QCM-D technique, it is noted that the $d\Delta\lambda/dt$ signal displays particularly high sensitivity to detect variations in adsorption-related protein denaturation.

By taking into account variations in solvent viscosity and the hydrodynamic diameter of solution-phase lysozyme proteins, which depend on the ethanol fraction in the water-ethanol mixtures, we next calculated the diffusion-limited adsorption rate of contacting protein molecules that attached to the sensor surface based on the Stokes-Einstein equation (see Supplementary Material for calculation details). This theoretically computed diffusion-limited adsorption rate was compared to the experimentally measured maximum adsorption rates obtained in the QCM-D and LSPR experiments and the normalized rate values are plotted together as a function of ethanol fraction in Fig. 7C.

In general, the theoretically calculated, diffusion-limited adsorption rate predicts that the normalized rate gradually decreases by up to around 50% as the ethanol fraction changes from 0% to 40%. Interestingly, in marked contrast, the QCM-D response shows an appreciable oscillatory trend in the normalized rate behavior, which coincides with the variation in protein hydrodynamic diameter [43] and exhibits an overall tendency towards greater rates by up to around 60% at higher ethanol fractions. This finding demonstrates that the conformational properties of the solution-phase lysozyme proteins play a critical role in dictating adsorption behavior, whereby increased levels of protein conformational flexibility at higher ethanol fractions enhance adsorption irreversibility *via* adsorption-related denaturation on the silica surface. This conformational effect is dominant over the dependence on solvent viscosity and the LSPR response shows a similar, albeit more modest, oscillatory trend in the normalized rate and a tendency towards rate increases up to around 30%. The difference in magnitudes of the normalized rate increases extracted from the QCM-D and LSPR measurement results further supports that variations in lysozyme conformational flexibility affect the hydrodynamic properties of lysozyme adlayers, which are detected in the QCM-D measurements.

3.6. Schematic summary of lysozyme adsorption trends

Fig. 8 presents a set of schematic illustrations that summarize lysozyme adsorption behavior in different water-ethanol mixtures. In 0% ethanol, lysozyme proteins have relatively low conformational flexibility (high conformational stability) and hence did not undergo extensive, adsorption-related denaturation. Upon solvent washing, the proteins remained irreversibly adsorbed due to strong protein-surface interactions that were mainly driven by attractive electrostatic forces and adlayer densification was negligible in this case due to the protein's relatively low conformational flexibility.

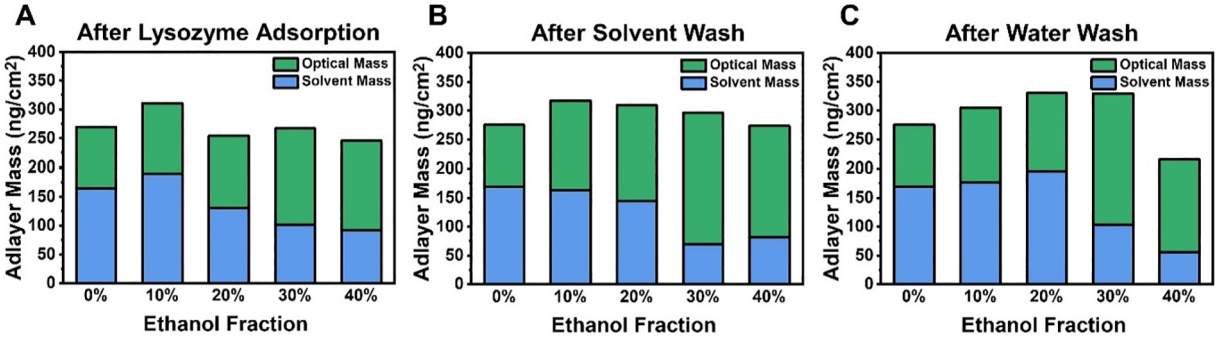

Fig. 6. Acoustic, optical, and solvent mass properties of lysozyme adlayers in water-ethanol mixtures. The acoustic, optical, and solvent mass values are reported for (A) lysozyme adlayer in water-ethanol mixture *before* solvent washing (relative to baseline in the appropriate water-ethanol mixture), (B) lysozyme adlayer in water-ethanol mixture *after* solvent washing (relative to baseline in the appropriate water-ethanol mixture), and (C) lysozyme adlayer *after* water washing (relative to baseline in water). Note that the acoustic mass is the sum of the optical and solvent mass values.

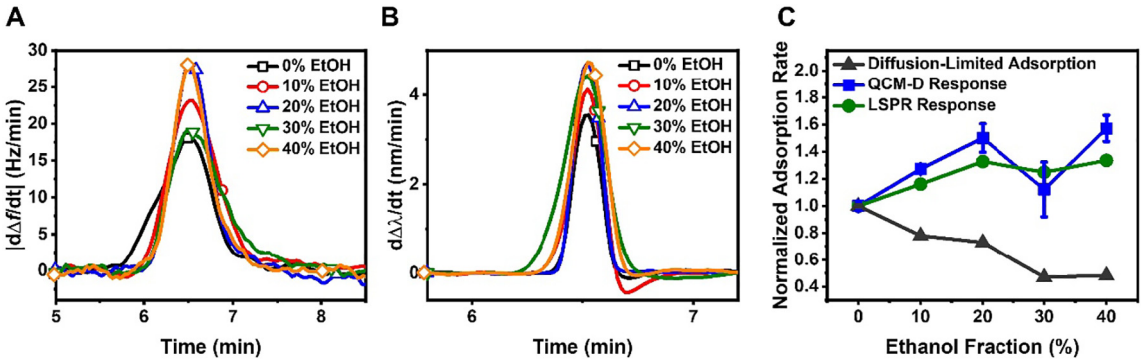

Fig. 7. Evaluation of lysozyme adsorption kinetics and theoretical comparison. Time derivative plots of the (A) $|\Delta f|$ and (B) $\Delta\lambda$ signals that were tracked during lysozyme adsorption in the QCM-D and LSPR experiments, respectively. (C) Comparison of the theoretically calculated, diffusion-limited adsorption rate and experimentally measured QCM-D and LSPR rates, which reflect the maximum values of the time derivatives of the Δf and $\Delta\lambda$ signals, respectively. The QCM-D data are reported as mean ± standard deviation (s.d.) for $n = 3$ replicates. In panel (C), all the presented rates are normalized whereby the rate value obtained in 0% ethanol was defined as 1 in each data set.

On the other hand, in water-ethanol mixtures with higher ethanol fractions, lysozyme proteins tend to exhibit greater conformational flexibility due to ethanol molecules solvating amino acid residues and disrupting intramolecular hydrophobic interactions [43,53,54]. In such cases, lysozyme proteins underwent greater adsorption-related denaturation and hence had stronger adsorption to the silica surface, which led to a higher degree of adsorption irreversibility. With increasing ethanol fraction, the resulting lysozyme adlayers therefore tended to have greater packing density and lower solvent mass amounts. Hence, lysozyme adlayer properties could be adjusted based on the ethanol fraction in the water-ethanol mixture used during the initial adsorption process and this finding establishes the broad importance of protein conformational tuning to modulate protein adsorption behavior.

4. Conclusions

In this study, we investigated the adsorption behavior of lysozyme proteins on silica surfaces in different water-ethanol mixtures and identified that solution-phase conformational stability plays a key role in dictating both adsorption kinetics and adlayer properties. A motivating factor behind this study was the unique conformational behavior of solution-phase lysozyme proteins in water-ethanol mixtures, whereby it has been noted that the hydrodynamic diameter of protein molecules tends to oscillate in magnitude with increasing ethanol fraction. This feature was attributed to non-monotonic variations in conformational stability – interpreted in terms of conformational flexibility – on account of competing water and ethanol solvation effects and is quite distinct from the conformational properties of other well-known proteins such as BSA in water-ethanol mixtures. Building on this knowledge, our experimental results demonstrate that lysozyme adsorption behavior also strongly depends on the ethanol fraction in a non-monotonic fashion and advances the importance of solution-phase conformational stability in dictating adlayer properties. By conducting QCM-D and LSPR measurements, it was possible to determine the adsorbed protein mass and hydrodynamically coupled solvent mass, which led us to identify that the hydrodynamic properties of lysozyme adlayers are mainly influenced by the degree of protein conformational flexibility as opposed to solvation effects alone. These findings have broad implications

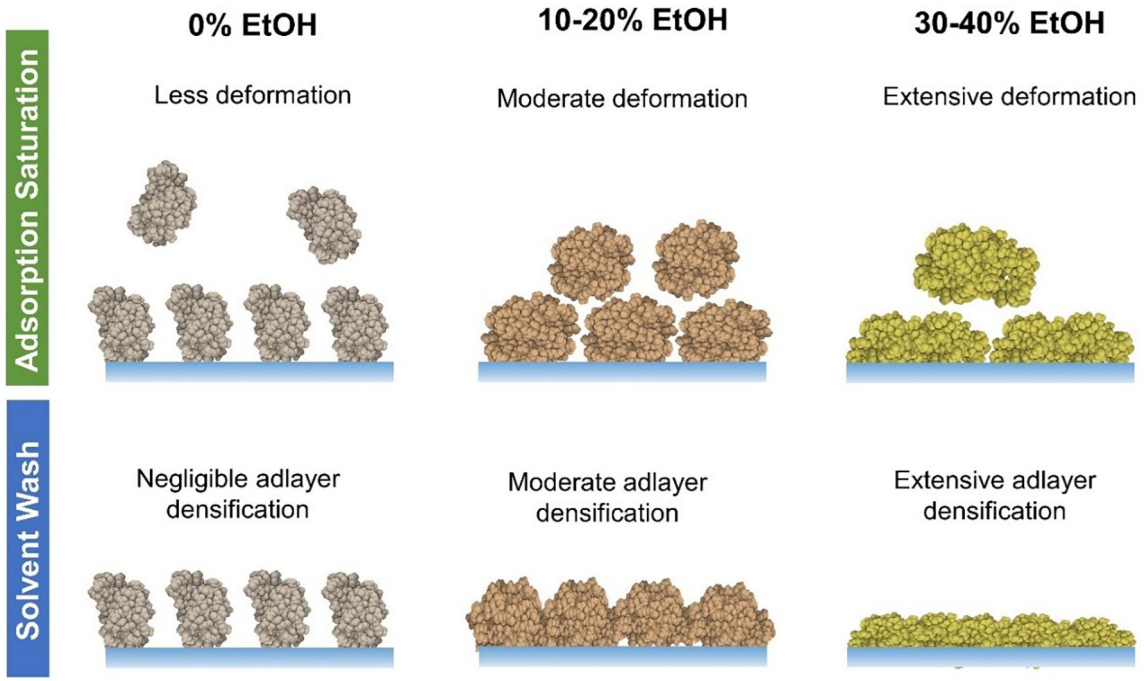

Fig. 8. Schematic illustration of lysozyme adsorption behavior in different water-ethanol mixtures. At higher ethanol fractions, solution-phase lysozyme proteins exhibited greater conformational flexibility (lower conformational stability) and hence underwent more extensive, adsorption-related denaturation and spreading on the silica surface. Upon solvent washing to remove weakly adsorbed protein molecules, significant adlayer densification was observed in water-ethanol mixtures with ≥10% ethanol fraction.

for designing improved protein-based coatings based on tuning the solution-phase conformational stability of proteins and could be applied to enhance the functional performance of lysozyme-based coatings.

CRediT authorship contribution statement

Bo Kyeong Yoon: Conceptualization, Methodology, Investigation, Writing - original draft, Visualization, Writing - review & editing. **Gamaliel Junren Ma:** Conceptualization, Methodology, Investigation, Writing - original draft, Visualization, Writing - review & editing. **Hyeonjin Park:** Methodology, Investigation, Writing - review & editing. **Abdul Rahim Ferhan:** Methodology, Analysis, Writing - review & editing. **Nam-Joon Cho:** Conceptualization, Writing - review & editing, Supervision. **Joshua A. Jackman:** Conceptualization, Methodology, Formal Analysis, Writing - original draft, Writing - review & editing, Resources, Supervision, Funding acquisition.

Declaration of competing interest

The authors declare that they have no known competing financial interests or personal relationships that could have appeared to influence the work reported in this paper.

Acknowledgements

This work was supported by the National Research Foundation of Korea (NRF) grant funded by the Korean government (MSIT) (No. 2020R1C1C1004385). In addition, this work was supported by the Brain Pool Program through the National Research Foundation of Korea (NRF) funded by the Ministry of Science and ICT (2019H1D3A1A01070318). Graphical illustrations were created with BioRender.com under an academic lab subscription.

Appendix A. Supplementary data

Supplementary data to this article can be found online at https://doi.org/10.1016/j.ijbiomac.2021.05.113.

References

[1] J.S. del Río, O.Y. Henry, P. Jolly, D.E. Ingber, An antifouling coating that enables affinity-based electrochemical biosensing in complex biological fluids, Nat. Nanotechnol. 14 (12) (2019) 1143–1149.
[2] S. Gupta, C. Murthy, C.R. Prabha, Recent advances in carbon nanotube based electrochemical biosensors, Int. J. Biol. Macromol. 108 (2018) 687–703.
[3] C. Pinholt, R.A. Hartvig, N.J. Medlicott, L. Jorgensen, The importance of interfaces in protein drug delivery – why is protein adsorption of interest in pharmaceutical formulations? Expert Opin. Drug Deliv. 8 (7) (2011) 949–964.
[4] R. Cagliani, F. Gatto, G. Bardi, Protein adsorption: a feasible method for nanoparticle functionalization? Materials 12 (12) (2019) 1991.
[5] W. Feng, P. Ji, Enzymes immobilized on carbon nanotubes, Biotechnol. Adv. 29 (6) (2011) 889–895.
[6] T. Jesionowski, J. Zdarta, B. Krajewska, Enzyme immobilization by adsorption: a review, Adsorption 20 (5–6) (2014) 801–821.
[7] M. Rabe, D. Verdes, S. Seeger, Understanding protein adsorption phenomena at solid surfaces, Adv. Colloid Interf. Sci. 162 (1–2) (2011) 87–106.
[8] E.A. Vogler, Protein adsorption in three dimensions, Biomaterials 33 (5) (2012) 1201–1237.
[9] A.E. Nel, L. Mädler, D. Velegol, T. Xia, E.M. Hoek, P. Somasundaran, F. Klaessig, V. Castranova, M. Thompson, Understanding biophysicochemical interactions at the nano–bio interface, Nat. Mater. 8 (7) (2009) 543–557.
[10] K. Ariga, Q. Ji, T. Mori, M. Naito, Y. Yamauchi, H. Abe, J.P. Hill, Enzyme nanoarchitectonics: organization and device application, Chem. Soc. Rev. 42 (15) (2013) 6322–6345.
[11] M. Komiyama, T. Mori, K. Ariga, Molecular imprinting: materials nanoarchitectonics with molecular information, Bull. Chem. Soc. Jpn. 91 (7) (2018) 1075–1111.
[12] B.E. Givens, Z. Xu, J. Fiegel, V.H. Grassian, Bovine serum albumin adsorption on SiO_2 and TiO_2 nanoparticle surfaces at circumneutral and acidic pH: a tale of two nano-bio surface interactions, J. Colloid Interface Sci. 493 (2017) 334–341.
[13] M.P. Calatayud, B. Sanz, V. Raffa, C. Riggio, M.R. Ibarra, G.F. Goya, The effect of surface charge of functionalized Fe3O4 nanoparticles on protein adsorption and cell uptake, Biomaterials 35 (24) (2014) 6389–6399.
[14] I. Firkowska-Boden, X. Zhang, K.D. Jandt, Controlling protein adsorption through nanostructured polymeric surfaces, Adv. Healthc. Mater. 7 (1) (2018), 1700995.
[15] S. Schöttler, G. Becker, S. Winzen, T. Steinbach, K. Mohr, K. Landfester, V. Mailänder, F.R. Wurm, Protein adsorption is required for stealth effect of poly (ethylene glycol)- and poly(phosphoester)-coated nanocarriers, Nat. Nanotechnol. 11 (4) (2016) 372.
[16] C.M. Dobson, A. Šali, M. Karplus, Protein folding: a perspective from theory and experiment, Angew. Chem. Int. Edit. 37 (7) (1998) 868–893.
[17] D.F. Marruecos, D.K. Schwartz, J.L. Kaar, Impact of surface interactions on protein conformation, Curr. Opin. Colloid Interface Sci. 38 (2018) 45–55.
[18] Y.F. Yano, Kinetics of protein unfolding at interfaces, J. Phys. Condens. Matter 24 (50) (2012), 503101.
[19] M. Karlsson, J. Ekeroth, H. Elwing, U. Carlsson, Reduction of irreversible protein adsorption on solid surfaces by protein engineering for increased stability, J. Biol. Chem. 280 (27) (2005) 25558–25564.
[20] G.J. Ma, A.R. Ferhan, T.N. Sut, J.A. Jackman, N.-J. Cho, Understanding how natural sequence variation in serum albumin proteins affects conformational stability and protein adsorption, Colloids Surf., B 194 (2020), 111194.
[21] J.H. Park, T.N. Sut, J.A. Jackman, A.R. Ferhan, B.K. Yoon, N.-J. Cho, Controlling adsorption and passivation properties of bovine serum albumin on silica surfaces by ionic strength modulation and cross-linking, Phys. Chem. Chem. Phys. 19 (13) (2017) 8854–8865.
[22] J.A. Jackman, A.R. Ferhan, B.K. Yoon, J.H. Park, V.P. Zhdanov, N.-J. Cho, Indirect nanoplasmonic sensing platform for monitoring temperature-dependent protein adsorption, Anal. Chem. 89 (23) (2017) 12976–12983.
[23] G.J. Ma, A.R. Ferhan, J.A. Jackman, N.-J. Cho, Conformational flexibility of fatty acid-free bovine serum albumin proteins enables superior antifouling coatings, Commun. Mater. 1 (1) (2020), 45.
[24] G.J. Ma, A.R. Ferhan, J.A. Jackman, N.-J. Cho, Elucidating how different amphipathic stabilizers affect BSA protein conformational properties and adsorption behavior, Langmuir 36 (35) (2020) 10606–10614.
[25] J.Y.B. Tan, B.K. Yoon, G.J. Ma, T.N. Sut, N.-J. Cho, J.A. Jackman, Unraveling how ethanol-induced conformational changes affect bsa protein adsorption onto silica surfaces, Langmuir 36 (31) (2020) 9215–9224.
[26] H. Park, G.J. Ma, B.K. Yoon, N.-J. Cho, J.A. Jackman, Comparing protein adsorption onto alumina and silica nanomaterial surfaces: clues for vaccine adjuvant development, Langmuir 37 (3) (2021) 1306–1314.
[27] R. Zhang, L. Wu, T. Eckert, M. Burg-Roderfeld, M.A. Rojas-Macias, T. Lütteke, V.B. Krylov, D.A. Argunov, A. Datta, P. Markart, A. Guenther, B. Norden, R. Schauer, A. Bhunia, M.A. Enani, M. Billeter, A.J. Scheidig, N.E. Nifantiev, H.-C. Siebert, Lysozyme's lectin-like characteristics facilitates its immune defense function, Q. Rev. Biophys. 50 (2017), e9.
[28] M. Derde, V. Vié, A. Walrant, S. Sagan, V. Lechevalier, C. Guérin-Dubiard, S. Pezennec, M.F. Cochet, G. Paboeuf, M. Pasco, Antimicrobial activity of lysozyme isoforms: key molecular features, Biopolymers 107 (12) (2017), e23040.
[29] A. Beaussart, C. Retourney, F. Quilès, R.D.S. Morais, C. Gaiani, H.-P. Fiérobe, S. El-Kirat-Chatel, Supported lysozyme for improved antimicrobial surface protection, J. Colloid Interface Sci. 582 (2021) 764–772.
[30] P. Bayazidi, H. Almasi, A.K. Asl, Immobilization of lysozyme on bacterial cellulose nanofibers: characteristics, antimicrobial activity and morphological properties, Int. J. Biol. Macromol. 107 (2018) 2544–2551.
[31] C. Buruaga-Ramiro, S.V. Valenzuela, C. Valls, M.B. Roncero, F.J. Pastor, P. Díaz, J. Martinez, Development of an antimicrobial bioactive paper made from bacterial cellulose, Int. J. Biol. Macromol. 158 (2020) 587–594.
[32] S. Sarkar, K. Gulati, A. Mishra, K.M. Poluri, Protein nanocomposites: special inferences to lysozyme based nanomaterials, Int. J. Biol. Macromol. 151 (2020) 467–482.
[33] S. Das, M. Pabba, M.E. Dhushyandhun, C.R. Patra, Theranostic applications of lysozyme-based nanoparticles, in: A.K. Shukla (Ed.), Nanoparticles in Medicine, Springer, Singapore, Singapore 2020, pp. 1–23.
[34] G. Jackler, R. Steitz, C. Czeslik, Effect of temperature on the adsorption of lysozyme at the silica/water interface studied by optical and neutron reflectometry, Langmuir 18 (17) (2002) 6565–6570.
[35] K. Xu, M.M. Ouberai, M.E. Welland, A comprehensive study of lysozyme adsorption using dual polarization interferometry and quartz crystal microbalance with dissipation, Biomaterials 34 (5) (2013) 1461–1470.
[36] K. Kubiak-Ossowska, M. Cwieka, A. Kaczynska, B. Jachimska, P.A. Mulheran, Lysozyme adsorption at a silica surface using simulation and experiment: effects of pH on protein layer structure, Phys. Chem. Chem. Phys. 17 (37) (2015) 24070–24077.
[37] A.R. Ferhan, B.K. Yoon, W.-Y. Jeon, J.A. Jackman, N.-J. Cho, Unraveling how nanoscale curvature drives formation of lysozyme protein monolayers on inorganic oxide surfaces, Appl. Mater. Today 20 (2020), 100729.
[38] R. Zhang, N. Zhang, M. Mohri, L. Wu, T. Eckert, V.B. Krylov, A. Antosova, S. Ponikova, Z. Bednarikova, P. Markart, A. Günther, B. Norden, M. Billeter, R. Schauer, A.J. Scheidig, B.N. Ratha, A. Bhunia, K. Hesse, M.A. Enani, J. Steinmeyer, A.K. Petridis, T. Kozar, Z. Gazova, N.E. Nifantiev, H.-C. Siebert, Nanomedical relevance of the intermolecular interaction dynamics—examples from lysozymes and insulins, ACS Omega 4 (2) (2019) 4206–4220.
[39] L. Jin, W. Gao, C. Liu, N. Zhang, S. Mukherjee, R. Zhang, H. Dong, A. Bhunia, Z. Bednarikova, Z. Gazova, M. Liu, J. Han, H.-C. Siebert, Investigating the inhibitory effects of entacapone on amyloid fibril formation of human lysozyme, Int. J. Biol. Macromol. 161 (2020) 1393–1404.
[40] L. Jin, C. Liu, N. Zhang, R. Zhang, M. Yan, A. Bhunia, Q. Zhang, M. Liu, J. Han, H.-C. Siebert, Attenuation of human lysozyme amyloid fibrillation by ACE inhibitor captopril: a combined spectroscopy, microscopy, cytotoxicity, and docking study, Biomacromolecules 22 (5) (2021) 1910–1920.
[41] P. Sassi, G. Onori, A. Giugliarelli, M. Paolantoni, S. Cinelli, A. Morresi, Conformational changes in the unfolding process of lysozyme in water and ethanol/water solutions, J. Mol. Liq. 159 (1) (2011) 112–116.

[42] T. Magsumov, L. Ziying, I. Sedov, Comparative study of the protein denaturing ability of different organic cosolvents, Int. J. Biol. Macromol. 160 (2020) 880–888.
[43] S. Chattoraj, A.K. Mandal, K. Bhattacharyya, Effect of ethanol-water mixture on the structure and dynamics of lysozyme: a fluorescence correlation spectroscopy study, J. Chem. Phys. 140 (11) (2014), 115105.
[44] A.B. Dahlin, J.O. Tegenfeldt, F. Höök, Improving the instrumental resolution of sensors based on localized surface plasmon resonance, Anal. Chem. 78 (13) (2006) 4416–4423.
[45] W. Norde, J.P. Favier, Structure of adsorbed and desorbed proteins, Colloids Surf. A Physicochem. Eng. Asp. 64 (1) (1992) 87–93.
[46] M. van der Veen, W. Norde, M.C. Stuart, Electrostatic interactions in protein adsorption probed by comparing lysozyme and succinylated lysozyme, Colloids Surf., B 35 (1) (2004) 33–40.
[47] M.F. Cuddy, A.R. Poda, L.N. Brantley, Determination of isoelectric points and the role of pH for common quartz crystal microbalance sensors, ACS Appl. Mater. Interfaces 5 (9) (2013) 3514–3518.
[48] G. Sauerbrey, The use of quartz oscillators for weighing thin layers and for microweighing, Z. Phys. 155 (1959) 206–222.
[49] M.P. Jonsson, A.B. Dahlin, P. Jönsson, F. Höök, Nanoplasmonic biosensing with focus on short-range ordered nanoholes in thin metal films, Biointerphases 3 (3) (2008) FD30–FD40.
[50] A.R. Ferhan, J.A. Jackman, N.-J. Cho, Integration of quartz crystal microbalance-dissipation and reflection-mode localized surface plasmon resonance sensors for biomacromolecular interaction analysis, Anal. Chem. 88 (24) (2016) 12524–12531.
[51] A.R. Ferhan, B. Spackova, J.A. Jackman, G.J. Ma, T.N. Sut, J. Homola, N.-J. Cho, Nanoplasmonic ruler for measuring separation distance between supported lipid bilayers and oxide surfaces, Anal. Chem. 90 (21) (2018) 12503–12511.
[52] P. Komorek, E. Martin, B. Jachimska, Adsorption and conformation behavior of lysozyme on a gold surface determined by QCM-D, MP-SPR, and FTIR, Int. J. Mol. Sci. 22 (3) (2021) 1322.
[53] S. Sarkar, B. Biswas, P.C. Singh, Spectroscopic and molecular dynamics simulation study of lysozyme in the aqueous mixture of ethanol: insights into the nonmonotonic change of the structure of lysozyme, J. Phys. Chem. B 122 (32) (2018) 7811–7820.
[54] W. Liu, D. Bratko, J.M. Prausnitz, H.W. Blanch, Effect of alcohols on aqueous lysozyme–lysozyme interactions from static light-scattering measurements, Biophys. Chem. 107 (3) (2004) 289–298.